LBL-10183
Preprint

Lawrence Berkeley Laboratory
UNIVERSITY OF CALIFORNIA

Materials & Molecular
Research Division

Submitted to the Journal of Chemical Physics

ISOTOPE, ELECTRIC FIELD, AND VIBRATIONAL STATE DEPENDENCE OF SINGLE ROTATIONAL LEVEL LIFETIMES OF S_1 FORMALDEHYDE

James C. Weisshaar and C. Bradley Moore

December 1979

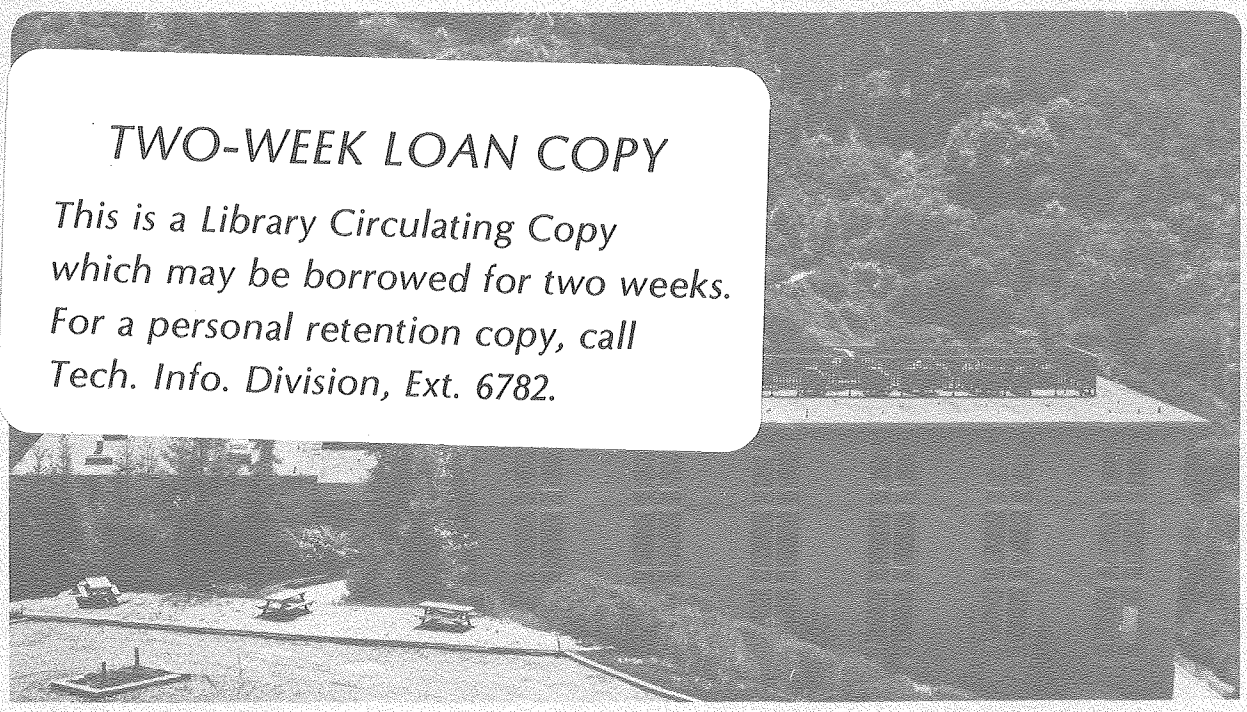

Prepared for the U.S. Department of Energy under Contract W-7405-ENG-48

DISCLAIMER

ISOTOPE, ELECTRIC FIELD, AND VIBRATIONAL STATE DEPENDENCE OF SINGLE ROTATIONAL LEVEL LIFETIMES OF S_1 FORMALDEHYDE

James C. Weisshaar[a] and C. Bradley Moore
Department of Chemistry, University of California,
and Materials and Molecular Research Division of
the Lawrence Berkeley Laboratory, Berkeley CA 94720

(Received)

Additional single rovibronic level lifetimes of S_1 H_2CO and D_2CO have been measured under collisionless conditions. The H_2CO 4^1 lifetimes vary at least a factor of 150, from 20 nsec to 3.10 μsec. The observed D_2CO 4^1 lifetimes fluctuate about ± 20% around a mean value of 6.2 μsec, which is probably close to the pure radiative lifetime. In contrast, the observed D_2CO 4^3 lifetimes vary from 1.09 to 2.46 μsec and the $2^1 4^3$ lifetimes vary from 212 nsec to 1.61 μsec. The onset of rotational state lifetime fluctuations in D_2CO thus coincides with the high pressure D_2 + CO photochemical threshold. All of these results are explained in terms of a collisionless sequential decay mechanism, $S_1 \rightarrow S_0 \rightarrow H_2(D_2)$ + CO. The last step probably involves tunneling through a barrier for the lower energies studied. For several H_2CO 4^1 rotational levels application of a uniform external electric field of 0 - 4.6 kV/cm can change the fluorescence lifetime by at

least a factor of 4. This result is understood in terms of small ($\lesssim 0.05$ cm^{-1}) shifts in $S_1 - S_0$ energy spacings. Quantitative estimates of $S_1 - S_0$ intramolecular couplings, S_0 widths due to dissociation, and S_0 level spacings are derived in favorable cases.

I. INTRODUCTION

By now there is a long history of S_1 formaldehyde lifetime measurements.[1, 2] Discrepancies in the early results have led to further investigations at much lower pressures and with better excitation resolution. Unusual phenomena continue to appear. Dramatic curvature of Stern-Volmer plots has been observed below 0.1 Torr,[3] indicating that many of the early zero pressure extrapolations were inaccurate. Lifetimes measured at low pressure with partial rotational state selection have shown fluctuations within single vibronic bands.[3, 4] Similar behavior has been observed for the fluorescence quantum yield ϕ_f upon excitation of single rotational levels (SRL's) of various bands.[5, 6]

Most recently, we have undertaken a program of direct measurement of SRL lifetimes at formaldehyde pressures low enough to preclude significant collisional relaxation on the timescale of the S_1 decay. These bulb measurements and recent supersonic jet lifetime measurements[7] are complementary in the sense that different sets of rotational levels are accessible in a bulb or a jet.

The results for the (vibrationless) 4^0 levels of H_2CO and D_2CO were reported in a previous paper.[8] The H_2CO 4^0 lifetimes fluctuate a remarkable factor of 50 or more with

rotational state, while the D_2CO lifetimes are uniform and essentially radiative. The present paper reports further SRL lifetime measurements for the H_2CO 4^1 level and for the D_2CO 4^1, 4^3, and $2^1 4^3$ levels. (The vibrations involved are ν_4, the out-of-plane bend of the hydrogens, and ν_2, the CO stretch). The new technique of monitoring changes in SRL fluorescence decay as a function of the external electric field strength[9] is shown to provide quantitative information about S_1 - S_0 couplings, S_0 widths due to dissociation, and S_0 level spacings in several cases of 4^1 excitation of H_2CO. There is clear evidence that the continuum of broadened S_0 levels coupled to S_1 is locally quite "lumpy," in that level spacings frequently exceed widths.

In the following, new experimental details, particularly of the electric field studies, are described in Sec. II. The SRL lifetime results for H_2CO and D_2CO are presented in Sec. III. Section IV gives previously unpublished details of the H_2CO 4^1 electric field results.[9] Section V is a discussion of our present understanding of the collision free decay mechanism of S_1, including the extraction of quantitative information from the electric field work. The discussion section of a previous paper[8] provides needed background. Finally, Sec. VI summarizes the present conclusions, points out major remaining questions, and suggests future experiments.

II. EXPERIMENTAL

The experiments involve measurement of the decay of H_2CO or D_2CO fluorescence from a static gas cell after pulsed dye laser excitation of single rotational levels of low-lying S_1 vibronic levels. The sample handling, the dye laser, the detection system, and signal processing, etc., have been described in detail.[3, 8] Fluorescence excitation spectra were obtained and assigned as before.[8] The same spectroscopic notation will be used here.

Zero-field lifetimes (Sec. III) were obtained in the fluorescence cell described previously.[8] A new fluorescence cell was built for lifetime measurements in the presence of a uniform, static electric field (Sec. IV). The main body of the glass cell is a cylinder 12 cm in diameter and 20 cm high, with a removable lid having a ground glass lip sealed with black wax (Apiezon W). The laser enters and exits the cell through two horizontal, 12 cm long, 2 cm diam arms having quartz Brewster windows. The lid and the bottom of the cell contain glass to metal seals to 1/4 in. diam, 4 cm long pieces of polished Kovar, to which ground and high voltage connections are made. The two polished stainless steel Stark electrodes are each disk-shaped, 10 cm in diam and ~ 1 cm thick, with rounded edges and a 1/4 in. diam stem. The electrode faces are flat to ± 0.001 cm. The bottom (high voltage) electrode is supported by the lower piece of Kovar into which its stem is threaded. Three quartz spacers of

thickness 1.279 ± 0.003 cm fix the electrode gap. The upper (ground) electrode rests on the spacers and is connected to the upper piece of Kovar with a wire.

Fluorescence at 90° to the laser is viewed through a 3 cm diam window by the photomultiplier tube placed at a distance that restricts its view to the central 8 cm of the space between electrodes to avoid edge effects. Field strengths of 0 - 4.6 kV/cm were applied via a regulated DC power supply. The applied voltages were measured to an accuracy of ± 2%. The electric field is uniform to better than ± 0.5% in the observation region. Wall effects are unimportant due to the sub-μsec lifetimes of the levels studied; zero field lifetimes agree well with those measured in the other cell. Scattered light intensity vs time is unaffected by the electric field, indicating that the detection electronics are not influenced. The Stark cell pumped down to $< 10^{-5}$ Torr; the leak/de-gas rate was 2×10^{-4} Torr per 10 min, the time required for a typical experiment.

For the present studies, red dye laser output was frequency doubled to give the necessary uv pulses. For the H_2CO 4_0^1 band and the D_2CO 4_0^1 and 4_0^3 bands (689 - 707 nm), a mixture of Rhodamine B and Nile Blue Nitrate was used. Concentration tuning of the gain curve and the use of a 60% R output coupler in the oscillator were helpful. For the D_2CO $2_0^1 4_0^3$ band (662 - 664 nm), a mixture of Rhodamine 6G and Cresyl Violet Perchlorate was used. The oscillator lases

on a single mode of an air-gap etalon (2 cm^{-1} FSR, nominal finesse 40). Pulse energies are typically 100 μJ in the red and 5 μJ in the uv. The uv linewidth, as evidenced by features in the fluorescence excitation spectrum, is 0.10 - 0.15 cm^{-1} FWHM, twice the Döppler width. The fluorescence amplitude follows the shot-to-shot laser intensity fluctuations of ~ 30%, indicating good frequency stability.

The photomultiplier viewed fluorescence through a uv cutoff filter (Schott KV 389, 50% T at 389 nm). Scattered light was a much less severe problem for these cold band studies than for the previous hot band (4_1^0) work.[8] Nevertheless, the detection-limited (7 nsec fall time) scattered light pulse was typically 2 - 5 times larger than the t = 0 signal amplitude at the low pressures studied and was carefully subtracted out to establish an accurate baseline.

III. ZERO FIELD LIFETIMES

For the H_2CO 4_0^1 band, the detailed assignments of Parkin[10] were useful in identifying lines and as a check of the excitation purity of a given line. Parkin's work is in excellent agreement with the absorption results of Dieke and Kistiakowsky[11] and with the electric field induced spectra of Bridge, Haner, and Dows.[12] The D_2CO 4_0^1, 4_0^3, and $2_0^1 4_0^3$ assignments are those of Job, Sethuraman, and Innes.[13, 14] Except as noted, only apparently clean, single rovibronic transitions were studied at pressures low enough to preclude significant collisional perturbation of the lifetimes. Single exponential decays over at least 1.5 decades were the rule under those conditions. Such lifetimes are accurate to ± 5%. The estimated maximum collisional perturbation[8] (based on a 1000 $\mathring{A}^2$ total inelastic cross-section)[3] is typically 1 - 10% of the measured lifetime and is included in the data tables. Clean excitation of single lines is much more difficult in the more crowded D_2CO bands than in H_2CO. For both isotopes, the blue edge of a band provides the best opportunity for clean excitation of strong, single lines.

A. H_2CO 4_0^1 Results

The present survey of H_2CO 4^1 lifetimes is less exhaustive than the earlier 4^0 study. Single exponential decays were observed for 32 different absorption features having K' in the range 0 - 9 and J' in the range 1 - 17. The results

are recorded in Table I. The pP_1, pQ_1, and rR_1 lines occur in the crowded center of the band, and Parkin's assignments[10] indicate that some apparently clean lines are in fact two or more overlapped transitions. These are noted in the table, along with calculated relative absorption intensities. In the cases for which two upper levels are strongly excited, the single exponential decay suggests that their lifetimes are similar.

Even in this small sample of 4^1 rotational states, the collisionless lifetime τ_0 varies a remarkable factor of 150, from 20 nsec to 3.10 μsec. A logarithmic plot of the decay rate τ_0^{-1} vs K' for various J' is shown in Fig. 1. As in 4^0, there is no smooth variation of τ_0^{-1} with J', K', or E_{rot} (the rotational energy) in 4^1. There is a strong average increase in decay rate with increasing K' or E_{rot}. This average trend is more accentuated in 4^1 than in 4^0. Lifetimes longer than 200 nsec are not observed for $K' \geq 4$, and the longest lifetimes ($\tau_0 > 1$ μsec) are observed only for $K' = 0$.

B. D_2CO 4_0^1 Results

The single exponential decay times measured at ten different wavelengths within the D_2CO 4_0^1 band are collected in Table II. The range of quantum numbers sampled is $J' = 3 - 18$, $K' = 2 - 5$. In several cases, more than one assigned transition was excited by the laser, yet a single exponential decay was observed. The lifetimes range from 5.0 μsec to 6.9 μsec

with a mean of 6.2 μsec. It is estimated that these lifetimes are collisionally perturbed by no more than about 10%, so the data indicate a slight variation of the collisionless decay rate with rotational state. A faster decay component was observed when the laser excited the overlapping transitions $rQ_2(6)$ and $rR_1(11)$, ν_{vac} = 28382.8 cm^{-1}, at a D_2CO pressure of 0.08 mTorr. In this case only, a biexponential decay with τ_f = 1.57 μsec, τ_s = 6.1 μsec, and I_f/I_s = 2.9 (ratio of fast to slow amplitude at t = 0) was observed. Such relatively fast decays are apparently quite unusual in 4^1 D_2CO.

C. D_2CO 4_0^3 Results

The D_2CO 4^3 lifetimes are faster and fluctuate more widely than the 4^1 lifetimes. The six single exponential decay rates reported in Table III range from 1.09 μsec to 2.46 μsec. Single exponential decays were common only at the less crowded blue edge of the band. In addition to the data of Table III, seven instances of non-exponential decay were observed, presumably due to spectral overlap of lines having different upper state lifetimes. When analyzed as biexponentials, these decays yield lifetimes similar to those of Table III.

The 4_0^3 band is of particular interest because Barnett, Ramsay, and Till[15] have observed and assigned magnetic rotation activity indicative of S_1 - T_1 perturbations for 13 rotational states. An attempt was made to selectively excite these levels in the hope of observing anomalous behavior.

In most cases, the appropriate lines are weak and/or overlapped by other transitions. Seven relatively favorable lines were studied, but the purity of excitation is questionable. Non-exponential decays were observed in all seven cases at a pressure of 0.2 mTorr. Interestingly, when these are analyzed as two exponential decays, the slow component lifetimes of 2.7 - 5.5 μsec are all slower than those of Table III, while the fast component lifetimes of 0.49 - 1.3 μsec are typically faster than those of Table III. The slow components are weak, and may well be associated with slight absorption contamination rather than with some T_1 non-radiative process.

D. D_2CO $2^1_0 4^3_0$ Results

For the $2^1 4^3$ level of D_2CO, single exponential decays were almost always observed; most of the lines studied were in the relatively uncrowded rR sub-bands. Occasionally two overlapped transitions were excited. The single exponential decay times are listed in Table IV. The lifetimes range from 212 nsec to 1.61 μsec, a variation of a factor of 8. It appears that states of higher K' (or E_{rot}) tend to have shorter lifetimes, although the sample of states is too small to strongly support this conclusion.

IV. ELECTRIC FIELD STUDIES

A. Spectroscopic Background

Both S_1 and S_0 H_2CO are nearly prolate tops. As the applied electric field increases from zero, a smooth transition, from a second-order to a first-order Stark effect occurs.[16] The effect is first order when the perturbation $-\mu EKM/J(J+1)$ is much larger than the K-doublet splitting Δ_{JK} of an asymmetry pair. This is typically the case for $K \geq 4$ for the fields of interest here. (See Table V of Ref. 8 for a list of S_1 splittings Δ_{JK}). As an example, for $J' = 5$, $K' = 4$ ($\Delta_{5,4} = 5 \times 10^{-7}$ cm^{-1}), the first-order limit certainly holds for fields E larger than 1 V/cm. The dipole moment μ is 1.56 D in S_1[18] and 2.33 D in S_0,[19] so that relative $S_1 - S_0$ energy spacings spacings can be tuned continuously by changing the electric field. The quantity $(\mu_{S_0} - \mu_{S_1})E$ is 1.29×10^{-5} cm^{-1} per (V/cm), so that relative shifts of at most 0.06 cm^{-1} occur in first order for the field strengths of 0 - 4600 V/cm used in this study. Second-order terms are about 10^2 smaller than the first-order term and are negligible when the latter does not vanish.

The dye laser was linearly polarized along the electric field direction, giving $\Delta M = 0$ absorption selection rules. The relative absorption intensities for the M components are proportional to M^2 for $\Delta J = 0$ (pQ and rQ) transitions and to

$(J'^2 - M^2)$ for $\Delta J = +1$ (rR) transitions.[18] The former case seems most favorable for seeing an effect, since the components that move the farthest in the field are most heavily weighted. Only for $K \sim J$ and for the largest fields employed here does the broadening of an absorption line due to the Stark splitting become comparable to the laser linewidth of 0.10 - 0.15 cm^{-1} FWHM. It is essentially the case that the laser excites all of the M-components at every field strength. The signal-to-noise ratio is poorer in these experiments than for the zero-field experiments of Sec. III because the viewing region of the photomultiplier tube must be severely restricted.

B. Results

A wide variety of behavior was observed for the nine H_2CO 4_0^1 transitions studied. For excitation of three of the most rapidly decaying SRL's having $\tau_0 \sim 25$ nsec, the fluorescence decay becomes non-exponential as the electric field is increased to a few kV/cm. The lines $rR_3(3)$, $rQ_3(10)$ and $rR_7(8)$ were studied at pressures of 2 - 3 mTorr. In all three cases, longer-lived (60 - 100 nsec) decay components grow in and there is evidence that some amplitude shifts towards faster ($\lesssim$ 20 nsec) components as well. Growth of longer-lived components is immediately obvious, whereas the concomitant growth of faster components is difficult to discern. It is possible to analyze the multi-exponential decay as a sum of only two exponentials in such a way that the slow

lifetime τ_s is a good estimate of the slowest decay component and the fast lifetime τ_f is an upper bound on the lifetime of the fastest component. This is done by intentionally skewing τ_s towards the longest time compatible with the data. This technique is used in Sec. V-C for the quantitative interpretation of these results.

Figure 2 shows the $rR_3(3)$ fluorescence decay for various applied voltages. By integrating the total area under a linear fluorescence intensity vs time curve, a quantity proportional to the M-averaged fluorescence lifetime can be obtained at each field strength. Each M-component is weighted according to its relative absorption intensity. Normalization of the area to the intensity at t = 0 corrects for any laser energy fluctuations. A single exponential decay can be used to fix the proportionality constant. The reciprocal of the M-averaged lifetime, $\langle\tau\rangle_M^{-1}$, is plotted vs electric field for the $rR_3(3)$ line in Fig. 1 of Ref. 9. Such plots are useful in that they characterize each multi-exponential decay by a single well-defined number, thus clearly showing trends in average lifetime.

For $rQ_3(10)$ and $rR_7(8)$, components as slow as 79 nsec (at 2340 V/cm) and 65 nsec (for $E \gtrsim 2340$ V/cm), respectively, grow in. Interestingly, for $rQ_3(10)$ the quantity $\langle\tau\rangle_M^{-1}$ decreases from 40 to 15 μsec^{-1} as the field increases from 0 to 2.3 kV/cm and then increases up to 22 μsec^{-1} at 4.6 kV/cm. The behavior at still higher fields might indicate that

resonance with a second S_0 level is beginning to occur.

Fluorescence from some lines studied clearly shifts towards faster decay rates with increasing electric field. For $rQ_3(7)$ at 2.0 mTorr the lifetime gradually shifts from τ_0 = 87 nsec to 52 nsec for 0 to 4.6 kV/cm; the decay remains essentially single exponential throughout. For $rR_3(5)$ at 1.6 mTorr, τ_0 = 160 nsec, the decay is non-exponential above about 800 V/cm. The slowest component shifts to ~ 120 nsec and comparable amplitude fast components having $\tau \lesssim 40$ nsec grow in. The quantity $\langle\tau\rangle_M^{-1}$ smoothly increases from 6 μs^{-1} to 13 μs^{-1} as the field changes from 0 - 4.6 kV/cm.

The two lines $rR_7(9)$ and $rR_7(10)$ showed no detectable change in fluorescence decay for fields of 0 - 4.6 kV/cm. The decays remained single exponential with lifetimes 41 ± 4 nsec and 35 ± 5 nsec, respectively, at a pressure of 3.2 mTorr.

Finally, two lines showed very sharp changes in the fluorescence decay with electric field. The case of $rQ_1(13)$ excitation has been described and illustrated previously.[9] For $rR_3(4)$ excitation, the zero field decay is essentially a single exponential with τ_0 = 125 nsec. (There is a small faster component of 20% relative amplitude which is probably due to slight contamination by the nearby $rR_3(9)$ line). At fields as small as 25 V/cm, the decay dramatically shifts towards faster components. The shift continues up to about 150 V/cm, beyond which the average decay gradually becomes

slower again. Figure 3 shows fluorescence decays vs Stark voltage while Fig. 4 shows $\langle\tau\rangle_M^{-1}$ vs voltage.

This small sample of experiments shows the wide variety of local environments in which 4^1 SRL's can be found. Section V-C discusses the extraction of quantitative information about S_1 - S_0 couplings, S_0 dissociative widths and S_0 level spacings from such experiments.

V. DISCUSSION

A. Collisionless Decay Mechanism

It is highly unlikely that discrete S_0 levels at ~ 29000 cm^{-1} are dense enough and strongly enough coupled to S_1 to result in a large molecule statistical limit such as that found in benzene or naphthalene.[20] (The density of S_0 vibronic levels near the S_1 origin is about 10 per cm^{-1} for H_2CO and 30 per cm^{-1} for D_2CO.[21]) As the only reasonable alternative, predissociation ($S_1 \rightarrow S_0 \rightarrow H_2 + CO$) is postulated to provide the necessary continuum of final states in the non-radiative decay of low-lying S_1 levels. The step $S_0 \rightarrow H_2 + CO$ may involve tunneling through a barrier to products.[22, 23] Observation of photofragments in a molecular beam would provide valuable experimental confirmation of this photochemical model.

Quantitative calculation of the decay rate of a particular S_1 SRL $|s\rangle$ thus requires construction of a set of S_0 rovibronic levels $|\ell\rangle$, each described by its energy E_ℓ, an $S_1 - S_0$ coupling matrix element $V_{s\ell}$, and a width Γ_ℓ due to dissociation. The essentially ab initio calculations of Heller, Elert, and Gelbart[24] represent a major effort along these lines. In the simple limit of weak coupling, $|V_{s\ell}| \ll |E_s - E_\ell - i\Gamma_\ell/2|$ for all ℓ, the decay of $|s\rangle$ is a single exponential whose rate is given by[25]

$$\Gamma_s^{nr} = (1/\hbar) \sum_\ell |V_{s\ell}|^2 \, \Gamma_\ell / [(E_s - E_\ell)^2 + (\Gamma_\ell/2)^2]. \qquad (1)$$

Experiment supports the validity of the weak coupling limit in that single exponential decays are consistently observed. The couplings $V_{s\ell}$ are dominated by vibronic terms;[26, 8] these are diagonal in J, K and M in a symmetric top basis set. Equation (1) shows that the major contribution to each Γ_s^{nr} comes from coupled S_0 levels that are nearly resonant with $|s>$. In the actual molecule, at least J and M are good quantum numbers so that each S_1 SRL is coupled to its own peculiar subset of S_0 rovibronic levels. Variations in $V_{s\ell}$, Γ_ℓ and $E_s - E_\ell$ thus contribute directly to variations in Γ_s^{nr}.

There are important questions about the nature of highly energetic S_0 levels. For example, if a harmonic oscillator basis is chosen,[21, 24] $S_1 - S_0$ matrix elements $V_{s\ell}$ and S_0 widths Γ_ℓ may vary over many orders of magnitude. But if anharmonic terms in the S_0 potential energy surface are "pre-diagonalized," the resulting basis set is more nearly a "molecular eigenstates" basis and variations of $V_{s\ell}$ and Γ_ℓ will be greatly diminished. A simplified model in which $V_{s\ell}$ and Γ_ℓ are essentially constant is the limiting case; variations in Γ_s^{nr} must then be attributed to "resonance effects" involving $(E_s - E_\ell)$ in the denominator of Eq. (1).

There are reasons to believe that K is a very poor quantum number at high energy in S_0, due to Coriolis (rotation vibration) coupling among many nearly degenerate rovibronic levels.[8] Such K-mixing can increase the density of levels vibronically coupled to S_1, dilute the $S_1 - S_0$ matrix elements

compared to those for a harmonic oscillator basis, and further diminish variations in $V_{s\ell}$ and Γ_{ℓ}. On the average, no increase in S_1 decay rate results, because the larger number of coupled levels is canceled by the dilution effect on $V_{s\ell}$. Analysis of S_0 high resolution vibration-rotation spectra[27] suggests that off-diagonal Coriolis couplings between K and K ± 1 on the order of 1 cm^{-1} are common; top asymmetry gives $\Delta K = \pm 2$ mixing in addition. In the limit of extreme mixing, the S_0 rovibronic levels would still divide into four sets of different symmetry species under the molecular point group C_{2v}. Each S_1 level would interact with the set of S_0 levels having appropriate J, M, and symmetry species. The density of such levels would be about $(2J' + 1)\ \rho_{vib}/4$, where ρ_{vib} is the vibrational level density. This is similar to an RRKM-like limit in which energy is statistically distributed among the vibrations and the K rotational degree of freedom.

A related question involves the "shape" of the S_0 continuum. The calculations of Yeung and Moore[28] assumed that each S_0 level was broadened by dissociation to the point of overlap with adjacent levels, providing a "smooth" continuum. SRL lifetime fluctuations might still be explained by wide variations in $V_{s\ell}$. The opposite limit is one in which S_0 widths are small compared to spacings, so that the continuum is "lumpy." Or both types of behavior may occur in limited energy regimes. Information about all of these points is beginning to emerge.

B. H_2CO Behavior

4^0 and 4^1 levels. It is reasonable to conclude[8] that the longest 4^0 and 4^1 SRL lifetimes observed, 4.2 μsec and 3.1 μsec, respectively, are essentially the radiative lifetimes of these vibronic levels. The $4^1/4^0$ ratio of 0.74 ± 0.07 agrees well with the ratio of radiative lifetimes of 0.68 ± 0.12 derived by Shibuya, et al.[29] from fluorescence intensities. The vast majority of the SRL lifetimes are much shorter than radiative.

The 4^1 Stark experiments, especially those revealing sharp edges on the plots of $\langle\tau\rangle_M^{-1}$ vs electric field, show that the continuum of S_0 levels coupled to S_1 is locally "lumpy" in the vicinity of the 4^0 and 4^1 levels. A picture in which S_0 widths or S_1 - S_0 couplings exceed level spacings is inappropriate here. Section V-C discusses further details.

For $K' > 3$, 25 - 100 nsec lifetimes are typical for 4^1 while 80 - 250 nsec lifetimes are typical for 4^0. The 4^0 and 4^1 inversion doublets are separated by only 125 cm^{-1} of vibrational energy compared with a range of about 0 - 1000 cm^{-1} of E_{rot} in these studies. The faster 4^1 decays are thus attributed to larger typical values of $|V_{s\ell}|^2$, by roughly a factor of 3. This corresponds to the notion that S_1 - S_0 Franck-Condon factors should increase with additional quanta of ν_4'.[28]

In 4^0 and especially in 4^1, the SRL decay rate increases on the average with increasing E_{rot} or K'. The S_0 vibrational

level density and the average S_1 - S_0 matrix element should not change over the range of energies studied. An explanation in terms of increased widths Γ_ℓ of the levels coupled to S_1 as E_{rot} or K' increases is therefore sought. This would also explain why the longest lifetimes are not observed for large E_{rot} or K'; as the S_0 widths increase, open spaces between levels become rare. Miller's[23] tunneling model for the widths Γ_ℓ is of interest in this context. The S_0 vibrational states are treated statistically and the reaction coordinate is assumed separable in this RRKM-like approach.

If K is a fairly good quantum number in S_0, then such a model predicts slower decay of S_1 SRL's as J' and K' increase. This is because the S_0 (and transition state)[22] rotational constants are larger than those of S_1. Increases in J' or K' require conversion of S_1 electronic energy into S_0 rotational energy (since J and K are conserved), leaving less energy available for the reaction coordinate. Typical Γ_ℓ's will decrease as J' and K' increase. If K is a good quantum number in S_0, the data require a model in which Γ_ℓ explicitly increases with K.

The opposite point of view asserts that K is a very poor quantum number in S_0. In the extreme case the "K-content" of each S_0 level becomes microcanonical, i.e., each K having $|K| \leq J'$ is equally likely. The rotational energy of such a level depends only on J and can be calculated easily. Various S_1 $J'K'$ SRL's either add to or diminish the energy available

to the vibrational degrees of freedom in S_0 (including the reaction coordinate) according to whether $E_{rot}^{S1}(J', K')$ is smaller or larger than the S_0 rotational energy for the same J. The separability assumption is retained. Such a model predicts the largest Γ_ℓ's for the case $J' \sim K' >> 0$ and the smallest Γ_ℓ's for $J' >> K' \simeq 0$, which is different from a simple trend of increasing decay rate with K' or E_{rot}. The data do not conclusively support this model. The large fluctuations in τ_0^{-1} due to $S_1 - S_0$ resonance effects make it difficult to separate possibly simple trends in Γ_ℓ with K' or E_{rot}. An absorption spectrum of high rovibrational levels of S_0 might shed light on the issue of K-conservation.

Shibuya and Lee[6] have recently reported absolute fluorescence quantum yield (ϕ_f) measurements for individual rR_3 lines of 4_0^1 H_2CO at 40 mTorr. Variations qualitatively similar to (but of smaller magnitude than) those of the direct τ_0 measurements were found. For the cases rR_3 (3, 4 and 9) for which clean excitation of a single line appears possible, the value $\tau_{rad} = 3$ μsec is used to convert the present lifetime measurements into ϕ_f values. Such derived values are uniformly 2 - 3 times smaller than those of Shibuya and Lee. Rotational relaxation at 40 mTorr may cause transfer to longer-lived SRL's and affect the comparison. The ϕ_f measurements were calibrated to an assumed value of 1.0 for D_2CO 4^1 at 5 mTorr; direct lifetime measurements suggest that 0.7 is a better estimate.[3]

Higher vibronic levels. Other workers have obtained information about SRL behavior in higher energy H_2CO vibronic levels. Tang, Fairchild, and Lee[5] report no significant variation of ϕ_f within the $2^2 4^1$ level (E_{vib} = 2500 cm^{-1}) with an accuracy of 20%. The H_2CO pressure was less than 0.2 Torr. Selzle and Schlag[7] have recently reported lifetimes of 18 $2^2 4^1$ SRL's for H_2CO expanded in a supersonic jet. Rotational levels having $J' = 0 - 5$ and $K' = 0 - 2$ were sampled. The lifetimes vary only from 6.1 to 9.9 nsec. The behavior of higher K' levels would be interesting. The agreement between the jet lifetimes and the earlier broadband $2^2 4^1$ lifetime of 9.8 nsec obtained by Miller and Lee[2] at 2 Torr in a bulb gives hope that such broadband, high pressure measurements provide a good indication of the collisionless behavior of higher H_2CO vibronic levels. The short, rather uniform lifetimes within $2^2 4^1$ are consistent with the idea that typical Γ_ℓ and $V_{s\ell}$ have increased at E_{vib} = 2500 cm^{-1}, due to faster $S_0 \rightarrow H_2 + CO$ decay (perhaps no longer requiring tunneling) and better $S_1 - S_0$ Franck-Condon factors[28]. Recent calculations show erratic fluctuations of average $V_{s\ell}$ as E_{vib} increases.[21, 30] The S_0 level density has changed very little over the same 2500 cm^{-1}. The continuum is apparently fairly smooth in this energy region. At still higher energy, experiments might show still smaller random variations of lifetimes with rotational state.

On the other hand, the SRL relative ϕ_f measurements of Tang, et al.[5] on the $2_0^3 4_0^1$ band of H_2CO (E_{vib} = 3600 cm^{-1}) show

fluctuations of a factor of 2 - 4. These were attributed to Coriolis coupling within S_1 to vibronic levels of different lifetime. Such vibronic lifetime variations due to $|V_{s\ell}|^2$ are not expected to wash out. An additional factor is the opening of the H + HCO channel for these higher levels. Stark experiments on such levels could directly test the local smoothness of the continuum.

C. Molecular Parameters from Stark Results

In favorable cases, quantitative estimates of particular molecular parameters such as $V_{s\ell}$, Γ_ℓ, and $E_s - E_\ell$ can be derived from the Stark experiments on 4^1 H_2CO SRL's. Difficulties arise from the excitation of all the M sub-levels, which leads to multi-exponential decays of total fluorescence, and from the unknown "K-content" of the interacting S_0 levels, which leads to uncertainty of a factor of 2 or so in the tuning of $E_s - E_\ell$ with electric field. No experimental information about these parameters was previously available, so that even order of magnitude estimates are quite useful. Comparisons with calculated values of $V_{s\ell}$[21, 30] and Γ_ℓ[23] are of interest.

The electric field perturbation $\underset{\sim}{\mu} \cdot \underset{\sim}{E}$ has A_2 symmetry in the C_{2v} point group.[34] Thus $\underset{\sim}{\mu} \cdot \underset{\sim}{E}$ and the nuclear kinetic energy T_N (which is totally symmetric) couple <u>different</u> sets of S_0 rovibronic levels to each S_1 rovibronic level. For fields up to 5 kV/cm, the inter-electronic matrix elements of $\underset{\sim}{\mu} \cdot \underset{\sim}{E}$ are at least 10^4 times smaller than average matrix

elements of T_N,[31] and are thus negligible in the present experiments. Furthermore, mixing of wavefunctions within S_1 by the field is a second-order effect; mixing coefficients are always smaller than 1%. The explanation of the large changes in fluorescence decay time with the Stark field must involve shifts in S_1 - S_0 level spacings.

For the $rR_3(4)$ case, we assume that $J' = 5$, $K' = 4$ interacts with $J'' = 5$, $K'' = 4$ S_0 levels. Then the dramatic shift in lifetime from 120 nsec to $\lesssim$ 20 nsec for fields of only 70 V/cm (see Sec. IV-B and Figs. 3 and 4) occurs for relative S_1 - S_0 energy shifts of only ~ 3×10^{-4} cm^{-1}. Furthermore, some 70% of the decay amplitude shifts and only gradually returns to slower components, suggesting that the S_1 level at zero field is in a narrow valley surrounded by at least two nearby S_0 levels. (For only one interacting level, if the $M < 0$ sub-levels shift towards resonance, the $M > 0$ sublevels shift away from resonance leading to longer-lived decay components which are not observed in this case). Referring to Eq. (1), the situation requires that $E_s - E_\ell$ and $\Gamma_\ell/2$ be $\lesssim 3 \times 10^{-4}$ cm^{-1} for some S_0 levels, or else the strong shift could not occur. Weak couplings $V_{s\ell}$ smaller than about 10^{-4} cm^{-1} are also necessary. Trial and error suggest that parameters such as $V_{s\ell} \sim 10^{-4}$ cm^{-1}, $\Gamma_\ell \sim 3 \times 10^{-4}$ cm^{-1} (corresponding to τ_{S_0} of 18 nsec) and two or three such weakly coupled levels within ~ 5×10^{-4} cm^{-1} could fit the data. The field rapidly tunes many M states into strong coupling with the nearby levels. The behavior is reminiscent of that of the 4^0 K-doublets,[8] for

which different lifetimes were observed in spite of S_1 splittings as small as 8×10^{-4} cm^{-1}.

The narrow resonance shape of $\langle\tau\rangle_M^{-1}$ for the $rQ_1(13)$ case[9] suggests that a single S_0 level tunes into and then out of resonance with the S_1 level excited. There is only a second-order Stark shift in S_1, while that of the interacting S_0 levels is not known. Detailed calculations show that unreasonably large second-order relative S_1 - S_0 Stark shifts are necessary to make the resonance broad enough in cm^{-1} to explain the fast components of ~ 250 nsec. Furthermore, most of the M sub-levels must shift into resonance essentially simultaneously, an effect that is difficult to obtain with either first or second-order S_0 Stark effects. An asymmetric lineshape which does not return to the baseline at high field is reminiscent of a perturbation which increases with the field. The interelectronic Stark couplings are much too small to explain the 250 nsec decay component, however. The origin of the unusual $rQ_1(13)$ lineshape is not simple.

For the cases in which the overall decay gradually shifts towards faster components, it is difficult to restrict the parameters. For $rR_7(9)$ and $rR_7(10)$, the two cases for which no change occurrred from 0 - 4.6 kV/cm, the suggestion is that the S_0 structure is quite uniform over local energy regions of ~ 0.02 cm^{-1} or more. The fast decay rates could be due to strong coupling ($V_{s\ell} \gtrsim 0.02$ cm^{-1}) to a nearby level of width $\Gamma_\ell \sim 3 \times 10^{-4}$ cm^{-1} ($\tau_{S_0} \sim 20$ nsec) or to weak coupling

($V_{s\ell} << E_s - E_\ell$) to broader, more distant ($E_s - E_\ell > 0.04\ cm^{-1}$) levels. A Doppler-free absorption spectrum could distinguish these possibilities.

A different approach was available for $rR_3(3)$. (See Fig. 2 and Fig. 1 of Ref. 9). At each field E, the slowest decay time was measured and is attributed to the M = 2 sub-level of $J' = 4$, $K' = 4$. (The absorption weighting is $16 - M^2$; although the $|M| = 3$ levels move the furthest, they are weak components). As shown in Fig. 5, the slowest decay rate $\Gamma_s(E)$ monotonically decreases a factor of 4 over the range 0 - 4.6 kV/cm, presumably because the M = 2 level moves out of resonance with a coupled S_0 level and encounters no other levels of comparable importance. Referring to Eq. (1), define $\delta_\ell(E) = E_s - E_\ell + \alpha E$ as the field-dependent $S_1 - S_0$ splitting, where α is a similar constant for all interacting S_0 levels. In the weak coupling limit, a field E can change an S_0 level's contribution to Γ_s only if it is "nearby," in the sense $(\alpha E)^2 \gtrsim \delta_\ell(0)^2 + (\Gamma_\ell/2)^2$. In the strong coupling limit $|V_{s\ell}| \gtrsim |E_s - E_\ell - i\Gamma_\ell|$, the field can change the contribution only if $(\alpha E)^2 \gtrsim |V_{s\ell}|^2$; the level has then moved out of the strong coupling regime.

Using such ideas, now assume that for the $rR_3(3)$ case, only one S_0 level contributes most of the width $\Gamma_s(E)$. Label that one level m. Equation (1) then leads to the usable result:

$$\Gamma_s(0)/\Gamma_s(E) = [(\delta_m(0) + \alpha E)^2 + (\Gamma_m/2)^2] \Big/ [(\delta_m(0)^2 + (\Gamma_m/2)^2], \tag{2}$$

where $\Gamma_s(0)/\Gamma_s(E)$ can be measured and αE can be calculated by assuming the coupled level has $J'' = K'' = 4$. The "one-state" assumption is supported (but hardly proved) by the fact that $\Gamma_s(0)/\Gamma_s(E)$ increases monotonically (as if no new resonances are encountered) by a factor of four (as if the nearby level dominates the zero-field decay rate).

Equation (2) is sensitive primarily to the ratio $2\delta_m(0)/\Gamma_m$. The off-resonance assumption $\delta_m(0)^2 >> (\Gamma_m/2)^2$ leads to a good fit of $\Gamma_s(0)/\Gamma_s(E)$, Fig. 5, and the measured $\Gamma_s(0)$ for the parameters $\delta_m(0) = 0.027\ cm^{-1}$, $V_{sm}^2\ \Gamma_m = 1.55 \times 10^{-7}\ cm^{-3}$. The off-resonance and weak coupling assumptions can separate V_m and Γ_m only to an extent: $0.002 < \Gamma_m < 0.02\ cm^{-1}$ and $0.009 > V_{sm} > 0.003\ cm^{-1}$.

A dead-resonant assumption $(\Gamma_m/2)^2 >> \delta_m(0)^2$ cannot fit the curvature of the data well. (See Fig. 5). The compromise assumption $\delta_m(0) = \Gamma_m/2$ can fit the data, and it results in the values $\delta_m(0) = 0.014\ cm^{-1}$, $V_{sm} = 1.7 \times 10^{-3}\ cm^{-1}$, and $\Gamma_m = 0.028\ cm^{-1}$, as shown in Fig. 5.

A strong coupling, "one-level" assumption leads to the estimates $\Gamma_m \simeq 4 \times 10^{-4}\ cm^{-1}$, $V_{sm} \simeq 5 \times 10^{-3}\ cm^{-1}$ and $\delta_m(0) \lesssim 5 \times 10^{-3}\ cm^{-1}$.

All of these limits lead to similar order of magnitude estimates: $V_{sm} \sim 5 \times 10^{-3}\ cm^{-1}$; $4 \times 10^{-4} < \Gamma_m < 3 \times 10^{-2}\ cm^{-1}$, corresponding to $13 > \tau_{S_0} > 0.2$ nsec; and $\delta_m(0) < 0.03\ cm^{-1}$. Similar parameters result from comparable analyses of the $rQ_3(10)$ and $rR_7(8)$ data. All the results

of this section must be viewed cautiously, of course, but they compare quite favorably with recent theoretical efforts. Elert[21] obtained a median $S_1 - S_0$ matrix element for 4^1 H_2CO of 7×10^{-3} cm^{-1}. Miller's S_0 lifetimes against tunneling[23] decrease from 300 nsec to 1 nsec as the vibrational energy increases from 2500 cm^{-1} below the barrier to the barrier height itself.

D. D_2CO Behavior

The discussion of Sec. VA applies to D_2CO as well. Again, the longest observed 4^0 and 4^1 SRL lifetimes, 8.1 and 6.9 μsec, are probably nearly radiative. The $4^1/4^0$ ratio of 0.85± 0.09 agrees well with the ratio of radiative lifetimes 0.82 ± 0.08 derived from fluorescence studies by Shibuya, et al.[32] The 4^0 and 4^1 SRL lifetimes fluctuate about 30%, presumably due to small non-radiative components. (Lifetime lengthening as an explanation of the longest lifetimes would require very large $S_1 - S_0$ total mixing coefficients of ~ 0.3). For 4^3 and $2^1 4^3$, the longest observed exponential decay times (Tables III and IV) are at least a factor of two shorter than the estimated radiative lifetimes.[2]

The primary motive for studying the 4^3 (E_{vib} = 669 cm^{-1}) and $2^1 4^3$ (E_{vib} = 1847 cm^{-1}) D_2CO SRL lifetimes was to see if larger lifetime fluctuations would begin to occur at energies corresponding to the opening of the D_2 + CO photochemical threshold at high pressure, 5 Torr. This is indeed the case.

The 4^3 lifetimes vary at least a factor of 2.5, while the $2^1 4^3$ lifetimes vary a factor of 8 or more. Earlier broadband work[1, 2] had already shown that the average D_2CO lifetime shortens dramatically as E_{vib} increases. Clark, et al.[33] have measured the absolute quantum yield of D_2 + CO photochemical products at 5 Torr after broadband excitation of various vibronic bands. A threshold behavior is observed. The equilibrated $4^0/4^1$ ($E_{vib} < 70$ cm^{-1}) average yield is 0.10 ± 0.10. The yield gradually rises to essentially one for $2^2 4^1$ ($E_{vib} = 2400$ cm^{-1}). Intermediate values of 0.30 for $2^1 4^1$ ($E_{vib} = 1244$ cm^{-1}) and 0.90 for $2^1 4^3$ were obtained. The agreement between the onset of D_2 + CO photochemistry and the onset of shorter, more widely fluctuating SRL lifetimes is taken as evidence that photochemistry is indeed the cause of the collisionless decay of S_1. Again, products have not yet been observed under isolated molecule conditions.

Several isotope effects can explain the much slower D_2CO non-radiative rate as compared to H_2CO at similar energy. The S_1 - S_0 matrix elements $V_{s\ell}$ are estimated to be at least 10 times smaller in D_2CO,[24, 30] essentially due to smaller Franck-Condon factors. Miller[23] finds that D_2CO tunnels more slowly than H_2CO by a factor that varies from 35 near the S_1 origin to 8 at about 2000 cm^{-1} above S_1. This comparison is between D_2CO and H_2CO rates at the same energy relative to their respective S_1 origins. In spite of the higher S_0 D_2CO level density, the widths and couplings are

apparently too small to permit photochemistry to compete with radiative decay at the S_1 origin. At higher energy, the non-radiative channel gradually becomes important. Eventually a "smooth continuum" limit should be reached.

IV. CONCLUSION

Much has been learned about the collisionless decay of H_2CO and D_2CO from low-lying S_1 SRL's. The emphasis is shifting from attempts to understand the basic mechanism towards efforts to obtain quantitative information about the molecular parameters (S_1 - S_0 matrix elements and S_0 widths and spacings) that determine decay rates. The new technique of Stark shifting the S_1 - S_0 level spacings[9] clearly demonstrates that the continuum of S_0 levels coupled to S_1 is characterized by levels well separated compared to their widths, at least near the S_1 origin. A smooth continuum model is not appropriate. Quantitative estimates of $V_{s\ell}$ in a few favorable cases indicate that recent calculations[21, 24] of S_1 - S_0 matrix elements of the nuclear kinetic energy using Herzberg-Teller theory give reasonable values. Estimates of a few S_0 widths are similar to recent tunneling calculations of the $S_0 \rightarrow H_2 + CO$ rate.[23] The tunneling mechanism permits fast non-radiative decay of S_1 even if the barrier to $H_2 + CO$ lies above the excited S_1 level, as is indicated by ab initio calculations.[22] There is a suggestion in the data that at least some memory of the initial K quantum number is preserved in S_0, and that the widths Γ_ℓ may increase with K as well as with total vibrational energy. For D_2CO, the fact that non-radiative decay and fluctuations in SRL lifetimes become important in the energy region of the high pressure $D_2 + CO$ photochemical threshold is strong evidence

that the non-radiative decay is due to photochemistry.

Electric field studies of additional 4^1 H_2CO SRL's, of higher H_2CO vibronic levels, and of D_2CO will provide further details about the nature of the S_0 continuum. The ultimate formaldehyde lifetime measurement will at least involve Doppler-free excitation of single $J'K'M'$ levels in the presence of an electric field. Such an M-selected experiment will avoid many of the complications encountered in the present work. Doppler-free absorption spectra could reveal details of the S_1 - S_0 couplings which are presently hidden; strong coupling vs weak coupling situations would be easily distinguished. Pressure dependent Stark experiments may be of interest in terms of the collisional decay of S_1.

ACKNOWLEDGMENTS

We thank M. L. Elert, R.W. Field, W.M. Gelbart, J.D. Goddard, D.F. Heller, E.K.C. Lee, W.H. Miller, H.F. Schaefer III, and A. Tramer for very helpful discussions. John Winn's expertise was essential in the design of the Stark cell. We gratefully acknowledge the research support of the Division of Advanced Systems Materials Production, Office of Advanced Isotope Separation, U.S. Department of Energy under contract No. W-7405-Eng-48 and the National Science Foundation. J.C.W. thanks the National Science Foundation for a predoctoral fellowship.

REFERENCES

[a] Present address: Joint Institute for Laboratory Astrophysics, University of Colorado, Boulder, CO 80309.

1. E.S. Yeung and C.B. Moore, J. Chem. Phys. 58, 3988 (1973).
2. R.G. Miller and E.K.C. Lee, J. Chem. Phys. 68, 4448 (1978) and references therein.
3. J.C. Weisshaar, A.P. Baronavski, A. Cabello and C.B. Moore, J. Chem. Phys. 69, 4720 (1978).
4. A.C. Luntz, J. Chem. Phys. 69, 3436 (1978).
5. K.Y. Tang, P.W. Fairchild, and E.K.C. Lee, J. Chem. Phys. 66, 3303 (1977).
6. K. Shibuya and E.K.C. Lee, J. Chem. Phys. 69, 5558 (1978).
7. H.L. Selzle and E.W. Schlag, Chem. Phys. 43, 111 (1979).
8. J.C. Weisshaar and C.B. Moore, J. Chem. Phys. 70, 5135 (1979).
9. J.C. Weisshaar and C.B. Moore, J. Chem. Phys., submitted for publication.
10. J.E. Parkin, Ph.D. Dissertation, University College, London (1962).
11. G.H. Dieke and G.B. Kistiakowsky, Phys. Rev. 45, 4 (1934).
12. N.J. Bridge, D.A. Haner, and D.A. Dows, J. Chem. Phys. 48, 4196 (1968).

13. V.A. Job, V. Sethuraman, and K.K. Innes, J. Mol. Spectrosc. 30, 365 (1969).

14. V. Sethuraman, V.A. Job, and K.K. Innes, J. Mol. Spectrosc. 33, 189 (1970).

15. M. Barnett, D.A. Ramsay and S.M. Till, Chem. Phys. Lett. 65, 440 (1979).

16. C.H. Townes and A.L. Schawlow, Microwave Spectroscopy (McGraw-Hill, New York, 1955).

17. N. Jannuzzi and S.P.S. Porto, J. Mol. Spectrosc. 4, 459 (1960).

18. D.E. Freeman and W. Klemperer, J. Chem. Phys. 45, 52 (1966).

19. K. Kondo and T. Oka, J. Phys. Soc. Jap. 15, 307 (1960). The calculated dipole moment for S_0 changes only about 10% from the equilibrium value when stretched to the transition state for $H_2CO(S_0) \rightarrow H_2 + CO$. Therefore the equilibrium value should give a reasonable approximation to the Stark tuning. (Private communication from authors of Ref. 22.)

20. P. Avouris, W.M. Gelbart and M.A. El-Sayed, Chem. Rev. 77, 794 (1977).

21. M.L. Elert, Ph.D. Dissertation, U.C. Berkeley (1978).

22. J.D. Goddard and H.F. Schaefer III, J. Chem. Phys. 70, 5117 (1979).

23. W.H. Miller, J. A. C. S., to be published.

24. D.F. Heller, M.L. Elert and W.M. Gelbart, J. Chem. Phys. 69, 4061 (1978).

25. A. Nitzan, J. Jortner and P.M. Rentzepis, Proc. Roy. Soc. London A327, 367 (1972); A. Nitzan and J. Jortner, Theor. Chim. Acta (Berlin) 29, 97 (1973).

26. F.A. Novak, S.A. Rice and K.F. Freed, Radiationless Transitions, edited by E. Lin (Academic, New York, 1979).

27. K. Yamada, T. Nakagawa, K. Kuchitsu and Y. Morino, J. Mol. Spectrosc. 38, 70 (1971); T. Nakagawa and Y. Morino, ibid., 84 (1971).

28. E.S. Yeung and C.B. Moore, J. Chem. Phys. 60, 2139 (1974).

29. K. Shibuya, R.A. Harger and E.K.C. Lee, J. Chem. Phys. 69, 751 (1978).

30. J.M.F. van Dijk, M.J.H. Kemper, J.H.M. Kerp and H.M. Buck, J. Chem. Phys. 69, 2462 (1978).

31. S.H. Lin, J. Chem. Phys. 62, 4500 (1975); W. Strek, Chem. Phys. Lett. 57, 121 (1978).

32. K. Shibuya, D.L. Holtermann, J.R. Peacock and E.K.C. Lee, J. Phys. Chem. 83, 940 (1979).

33. J.H. Clark, C.B. Moore and N.S. Nogar, J. Chem. Phys. 68, 1264 (1978).

34. J.T. Hougen, J. Chem. Phys. 37, 1433 (1962).

TABLE I. H_2CO 4^1 lifetimes. (E_{vib} = 125 cm^{-1}).

Line(s)[a]	J'	K'	Rot. Symm.[b]	E_{rot}[c] (cm^{-1})	ν_{vac}[a] (cm^{-1})	Pressure (mTorr)	τ(μs)[d]	τ^{-1}(μs^{-1})	%Coll. Pert.[e]
$pQ_1(1)$	1	0	(-+)	2.1	28304.0	0.1	2.66	0.376	5
$pP_1(2)$	1	0	(-+)	2.1	299.4	0.2	2.85	0.351	11
0.77 $pQ_1(3)$	3	0	(-+)	12.8	302.1	0.2	3.10	0.322	12
0.23 $pP_1(1)$	0	0	(++)	0.0					
0.74 $pQ_1(4)$	4	0	(++)	21.4	300.6	0.4	0.563	1.77	5
0.20 $rP_1(6)$	5	2	(++)	62.8					
0.38 $pQ_1(5)$	5	0	(-+)	32.1	298.7	0.7	0.409	2.44	6
0.33 $rQ_1(14)$	14	2	(++)	256.9					
0.29 $pR_2(9)$	10	1	(--)	128.4					

TABLE I. H_2CO 4^1 lifetimes. (E_{vib} = 125 cm^{-1}). (continued)

Line(s)[a]	J'	K'	Rot. Symm.[b]	E_{rot}[c] (cm^{-1})	ν_{vac}[a] (cm^{-1})	Pressure (mTorr)	τ(μs)[d]	τ^{-1}(μs^{-1})	%Coll. Pert.[e]
$rR_1(1)$	2	2	(++)	37.2	339.2	1.3	0.69	1.45	20
$rR_1(3)$	4	2	(-+)	52.1	341.4	1.3	0.487	2.05	13
0.62 $rR_1(6)$	7	2	(-+)	90.8	345.8	1.4	0.453	2.21	13
0.20 $rR_1(19)$	20	2	(++)	485.6					
$rR_1(7)$	8	2	(-+)	107.8	341.7	1.3	0.083	12.0	2
0.90 $rR_1(9)$	10	2	(-+)	148.4	339.7	1.3	0.067	14.9	2
0.10 $rQ_7(20)$	20	8	(±+)	940.3					
0.80 $rR_1(9)$	10	2	(++)	149.0	347.5	1.5	0.081	12.3	2
0.20 $rR_1(15)$	16	2	(++)	324.3					

TABLE I. H_2CO 4^1 lifetimes. (E_{vib} = 125 cm^{-1}). (Continued)

Line(s)[a]	J'	K'	Rot. Symm.[b]	E_{rot}[c] (cm^{-1})	ν_{vac}[a] (cm^{-1})	Pressure (mTorr)	τ(μs)[d]	τ^{-1}(μs^{-1})	%Coll. Pert.[e]
$rR_1(10)$	11	2	(++)	171.9	338.2	1.3	0.238	4.20	6
0.73 $rQ_1(13)$	13	2	(-+)	226.6	303.3	0.2	0.86	1.15	3
0.27 $pQ_1(2)$	2	0	(++)	6.4					
$rR_3(3)$	4	4	(±+)	144.3	368.5	1.5	0.025	40.0	0.8
$rR_3(4)$[f]	5	4	(±+)	155.0	369.4	1.2	0.113	8.9	3
$rQ_3(7)$[g]	7	4	(±+)	182.8	353.4	1.8	0.087	11.5	3
$rR_3(9)$	10	4	(±+)	240.4	369.7	2.1	0.027	37.0	1
$rR_6(9)$	10	7	(±-)	493.9	401.8	1.5	0.038	26.3	1
$rR_6(10)$	11	7	(±-)	517.5	400.9	1.5	0.069	14.6	2
$rR_6(11)$	12	7	(±-)	543.1	399.7	2.8	0.020	50.0	1

TABLE I. H_2CO 4^1 lifetimes. (E_{vib} = 125 cm^{-1}). (Continued)

Line(s)[a]	J'	K'	Rot. Symm.[b]	E_{rot}[c] (cm^{-1})	ν_{vac}[a] (cm^{-1})	Pressure (mTorr)	τ(μs)[d]	τ^{-1}(μs^{-1})	% Coll. Pert.[e]
$rR_6(12)$	13	7	(±-)	570.9	398.3	2.8	0.026	39.2	2
$rR_7(7)$	8	8	(±+)	568.7	411.1	1.8	0.047	21.5	2
$rR_7(8)$	9	8	(±+)	587.9	410.9	3.2	0.025	40.0	2
$rR_7(9)$	10	8	(±+)	609.3	410.4	2.1	0.041	24.6	2
$rR_7(10)$	11	8	(±+)	632.8	409.5	1.8	0.036	27.7	1
$rR_7(12)$	13	8	(±+)	686.2	406.9	1.5	0.058	17.4	2
$rR_7(13)$	14	8	(±+)	716.1	405.1	1.5	0.051	19.5	2
$rR_7(15)$	16	8	(±+)	782.3	400.7	1.5	0.070	14.2	2
$rR_7(16)$	17	8	(±+)	818.6	398.7	1.7	0.059	16.8	2
$rR_8(9)$	10	9	(±-)	739.9	417.9	1.5	0.113	8.9	3
$rR_8(11)$	12	9	(±-)	789.0	415.9	2.3	0.045	22.2	2
$rR_8(13)$	14	9	(±-)	846.7	412.7	2.2	0.033	30.3	2

TABLE I. H_2CO 4^1 lifetimes. (E_{vib} = 125 cm^{-1}). (continued)

a) The assignments are those of Parkin, Ref. 10. When more than one assignment occurs, relative absorption weights calculated from symmetric top wavefunctions are given for the major components.

b) The asymmetric top, rigid rotor symmetry species of the S_1 level.

c) Rigid rotor energies in S_1, obtained from App. IV, Ref. 16 or from Table I, Ref. 17.

d) Lifetimes are accurate to ± 5% (± 2 σ).

e) Estimated maximum % perturbation of lifetimes by collisions of 1000 $\mathring{A}^2$ cross section. See the beginning of Sec. III of the text.

f) There is a small (< 20% relative amplitude) faster component, probably due to slight excitation of $rR_3(9)$, which is nearby.

g) This lifetime was obtained at zero field in the Stark cell.

TABLE II. D_2CO 4^1 lifetimes. (E_{vib} = 69 cm^{-1}).

Line(s)[a]	J'	K'	Rot. Symm.[b]	ν_{vac}[a] (cm^{-1})	Pressure (mTorr)	τ(μs)[c]	τ^{-1}(μs^{-1})[c]	% Coll. Pert.[d]
$rQ_2(3)$	3	3	(±-)	28385.6	0.08	6.9	0.145	11
$rR_1(8)$	9	2	(++)					
$rR_2(14)$	15	3	(+-)	397.8	0.06	4.97	0.201	6
$rR_1(10)$	11	2	(-+)					
$rQ_3(4)$	4	4	(±+)	391.2	0.08	6.1	0.164	10
$rR_1(6)$	7	2	(-+)					
$rQ_3(10)$	10	4	(++)	382.0	0.08	6.9	0.145	11
$rR_3(13)$	14	4	(-+)	398.5	0.07	6.3	0.159	9
$rR_4(4)$	5	5	(±-)	406.0	0.06	6.5	0.154	8
$rR_4(12)$	13	5	(±-)	406.6	0.06	6.5	0.154	8

TABLE II. D_2CO 4^1 lifetimes. (E_{vib} = 69 cm^{-1}). (Continued)

Line(s)[a]	J'	K'	Rot. Symm.[b]	ν_{vac}[a] (cm^{-1})	Pressure (mTorr)	τ(μs)[c]	τ^{-1}(μs^{-1})[c]	% Coll. Pert.[d]
$rR_4(15)$	16	5	(+-)	403.2	0.08	5.00	0.200	8
$rR_4(15)$	16	5	(--)	403.5	0.08	6.3	0.159	10
$rR_1(13)$	14	2	(++)					
$rR_4(17)$	18	5	(+-)	399.5	0.10	6.8	0.147	14
$rR_1(11)$	12	2	(++)					

a) The assignments are those of Ref. 13. The brackets indicate cases of excitation of several assigned lines within the laser linewidth.

b) The asymmetric top, rigid rotor symmetry species of the S_1 level.

c) Lifetimes are accurate to ± 5% (± 2 σ).

d) See footnote e under Table I.

TABLE III. D_2CO 4^3 lifetimes. (E_{vib} = 669 cm^{-1}).

Line[a]	J'	K'	Rot. Symm.[b]	ν_{vac}[a] (cm^{-1})	Pressure (mTorr)	τ(μs)[c]	τ^{-1}(μs^{-1})[c]	% Coll. Pert.[d]
$rR_4(4)$	5	5	(±-)	29001.3	0.1	2.46	0.406	5
$rR_8(10)$	11	9	(±-)	015.4	0.2	1.97	0.507	8
$rR_8(11)$	12	9	(±-)	014.9	0.2	1.31	0.76	5
$rR_8(12)$	13	9	(±-)	014.3	0.2	1.09	0.91	4
$rR_8(13)$	14	9	(±-)	013.5	0.3	1.62	0.62	10
$rR_{10}(13)$	14	11	(±-)	016.8	0.4	1.79	0.557	14

a) The assignments are those of Ref. 14.

b) The asymmetric top, rigid rotor symmetry species of the S_1 level.

c) Lifetimes are accurate to ± 5% (± 2 σ).

d) See footnote e under Table I.

TABLE IV. D_2CO $2^1 4^3$ lifetimes. (E_{vib} = 1847 cm^{-1}).

Line(s)[a]	J'	K'	Rot. Symm.[b]	ν_{vac}[a] (cm^{-1})	Pressure (mTorr)	τ(μs)[c]	τ^{-1}(μs^{-1})[c]	% Coll. Pert.[d]
$pR_1(13)$	14	0	(++)	30154.6	0.2	1.13	0.89	4
$pR_1(8)$	9	0	(-+)					
$rR_0(9)$	10	1	(+-)	157.0	0.2	1.12	0.90	4
$rQ_6(14)$	14	7	(±-)					
$rR_0(11)$	12	1	(+-)	156.3	0.2	1.61	0.62	6
$rQ_1(3)$	3	2	(++)					
$rR_1(4)$[e]	5	2	(++)	162.7	0.2	1.06	0.94	4
$rR_1(9)$	10	2	(++)	171.7	0.5	0.89	1.12	9
$rR_5(5)$	6	6	(±+)	182.6	1.0	0.87	1.15	18
$rR_5(10)$	11	6	(±+)	182.9	1.0	0.81	1.24	16

TABLE IV. D_2CO $2^1 3^4$ lifetimes. (E_{vib} = 1847 cm^{-1}). (Continued).

Line(s)[a]	J'	K'	Rot. Symm.[b]	ν_{vac}[a] (cm^{-1})	Pressure (mTorr)	τ(μs)[c]	τ^{-1}(μs^{-1})[c]	% Coll. Pert.[d]
$rR_5(11)$	12	6	(±+)	182.3	2.5	0.212	4.72	10
$rR_6(12)$	13	7	(±-)	185.2	1.0	0.523	1.91	10
$rR_6(13)$	14	7	(±-)	184.4	1.3	0.504	1.98	13
$rR_6(15)$	16	7	(±-)	182.0	1.5	0.381	2.62	11
$rR_8(11)$	12	9	(±-)	190.6	0.9	0.510	1.96	9
$rR_9(9)$	10	10	(±+)	194.2	1.5	0.72	1.39	22
$rR_9(10)$	11	10	(±+)	193.7	1.6	0.452	2.21	14
$rR_{10}(10)$	11	11	(±-)	195.6	1.4	0.571	1.75	16
$rR_{10}(11)$	12	11	(±-)	195.0	1.6	0.552	1.81	18
$rR_{10}(12)$	13	11	(±-)	194.1	1.4	0.422	2.37	12

TABLE IV. D_2CO $2^1 3^4$ lifetimes. (E_{vib} = 1847 cm^{-1}). (Continued).

a) The assignments are those of Ref. 14.

b) The asymmetric top, rigid rotor symmetry species of the S_1 level.

c) Lifetimes are accurate to ± 5% (± 2 σ).

d) See footnote e under Table I.

e) This line may be somewhat contaminated by the strong nearby $rR_1(5,6)$ and $rQ_3(6)$ lines at 30162.9 cm^{-1}.

Figure 1. Logarithmic plot of H_2CO 4^1 SRL decay rate vs K'. The trend of increasing rate with K' is quite strong.

Figure 2. The decay of total fluorescence after 4_0^1, $rR_3(3)$ excitation of 2.2 mTorr of H_2CO for various applied voltages. Electric field strength can be obtained by dividing each voltage by 1.28 cm. The zero field lifetime is 25 nsec, while the slowest component at 5900 V is about 100 nsec, four times longer.

Figure 3. The decay of total fluorescence after 4_0^1, $rR_3(4)$ excitation of 2.3 mTorr of H_2CO for various applied voltages. The zero field decay is nearly a single exponential of lifetime 125 nsec. By 100 V, as much as 80% of the decay has shifted to faster components of lifetime $\lesssim$ 20 nsec.

Figure 4. Plot of the reciprocal of the M-weighted average lifetime for 4_0^1, $rR_3(4)$ excitation of H_2CO vs applied Stark voltage. See Sec. IV-B of the text.

Figure 5. The ratio of the decay rate at zero field to the slowest decay rate component at each electric field, plotted vs electric field for $rR_3(3)$, 4_0^1 excitation of H_2CO. The lines represent fits of the data to Eq. (2) under these assumptions: solid line, $\delta_m(0)^2 >> (\Gamma_m/2)^2$ and $\delta_m(0) = 0.027$ cm^{-1}; dashed line, (---), $(\Gamma_m/2)^2 >> \delta_m(0)^2$ and $\Gamma_m = 0.025$ cm^{-1}; broken line (— —), $\delta_m(0) = \Gamma_m/2 = 0.014$ cm^{-1}.

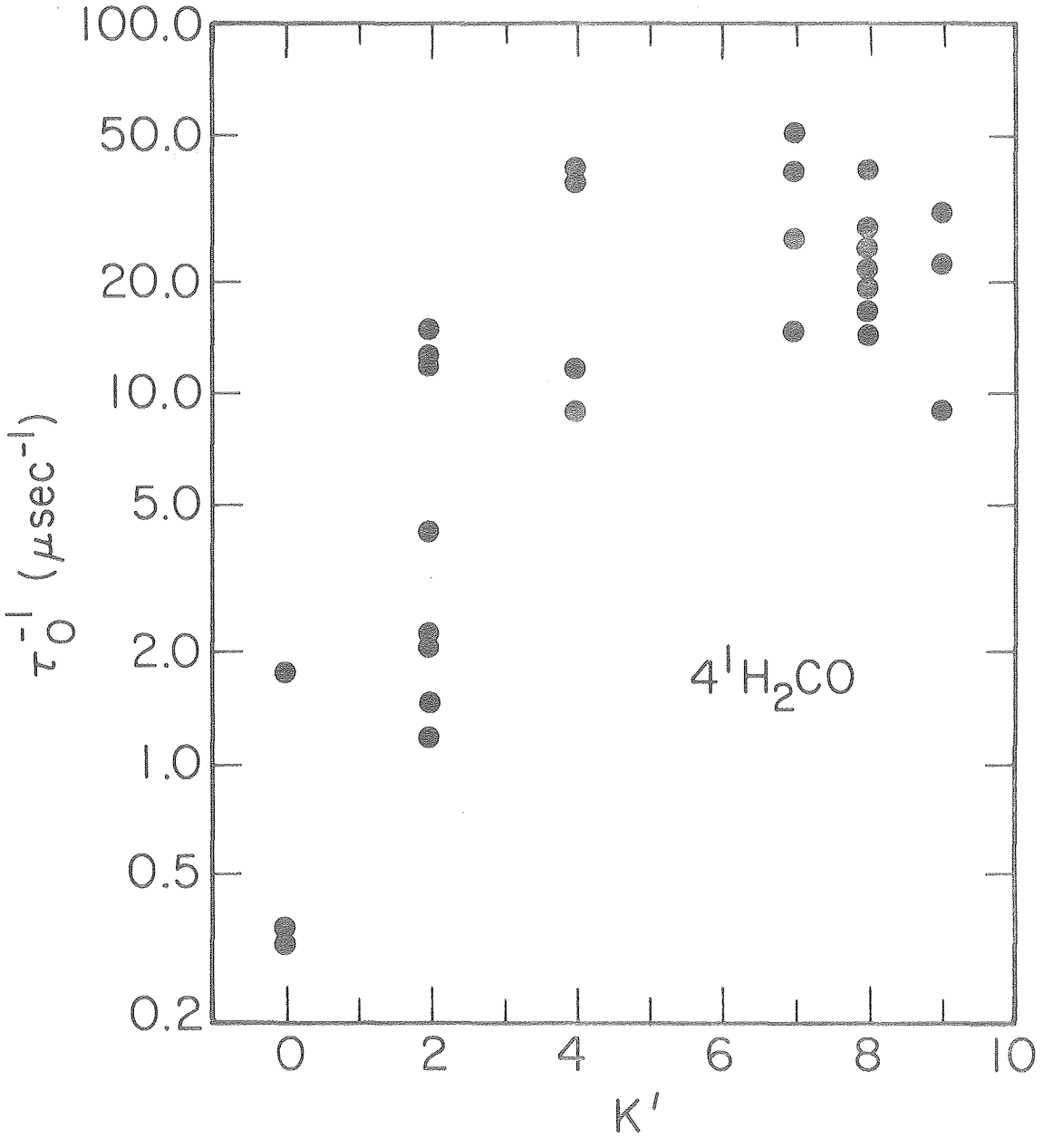

XBL 7911-12715

Fig. 1.

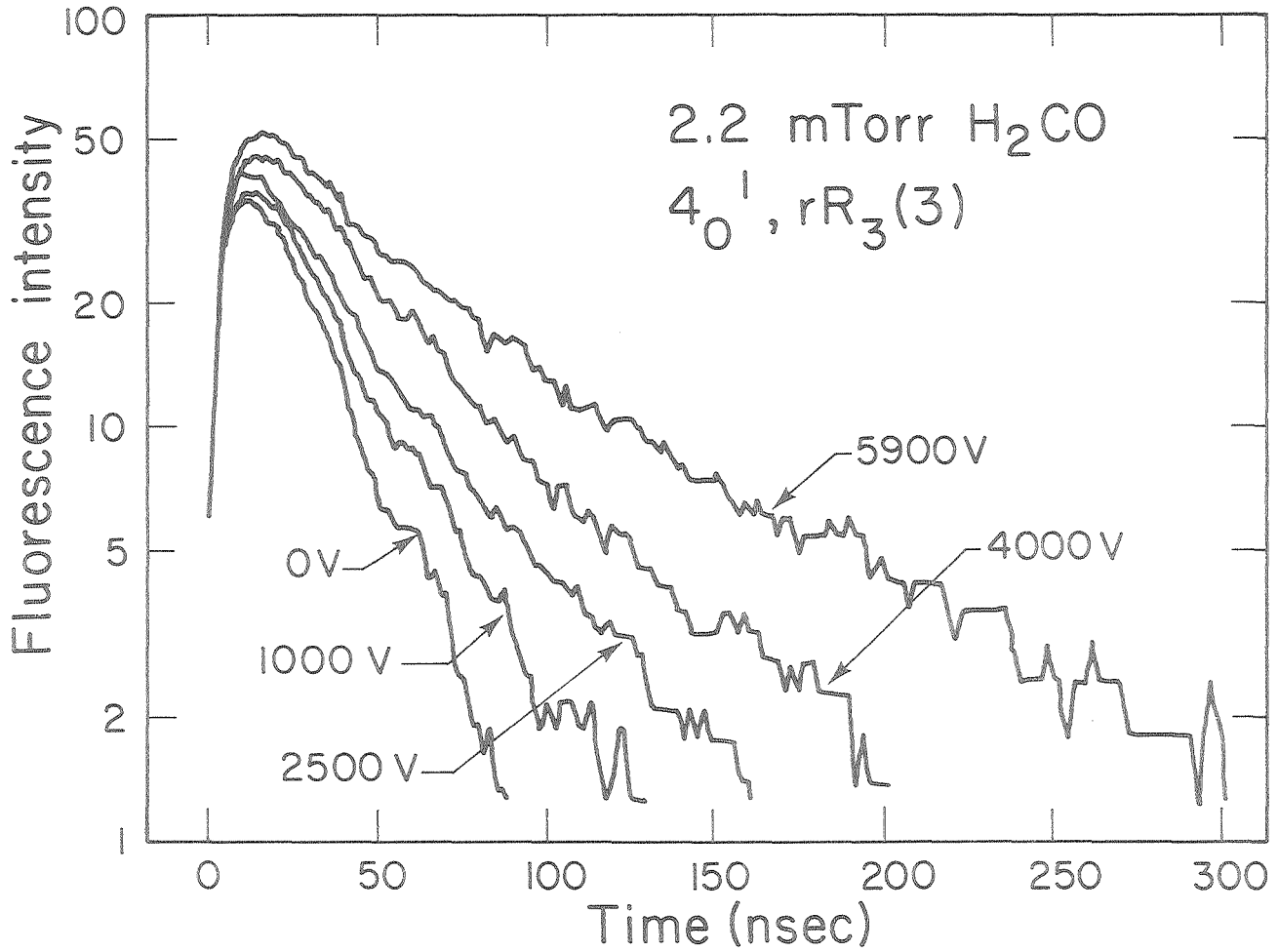

XBL 798-2715

Fig. 2.

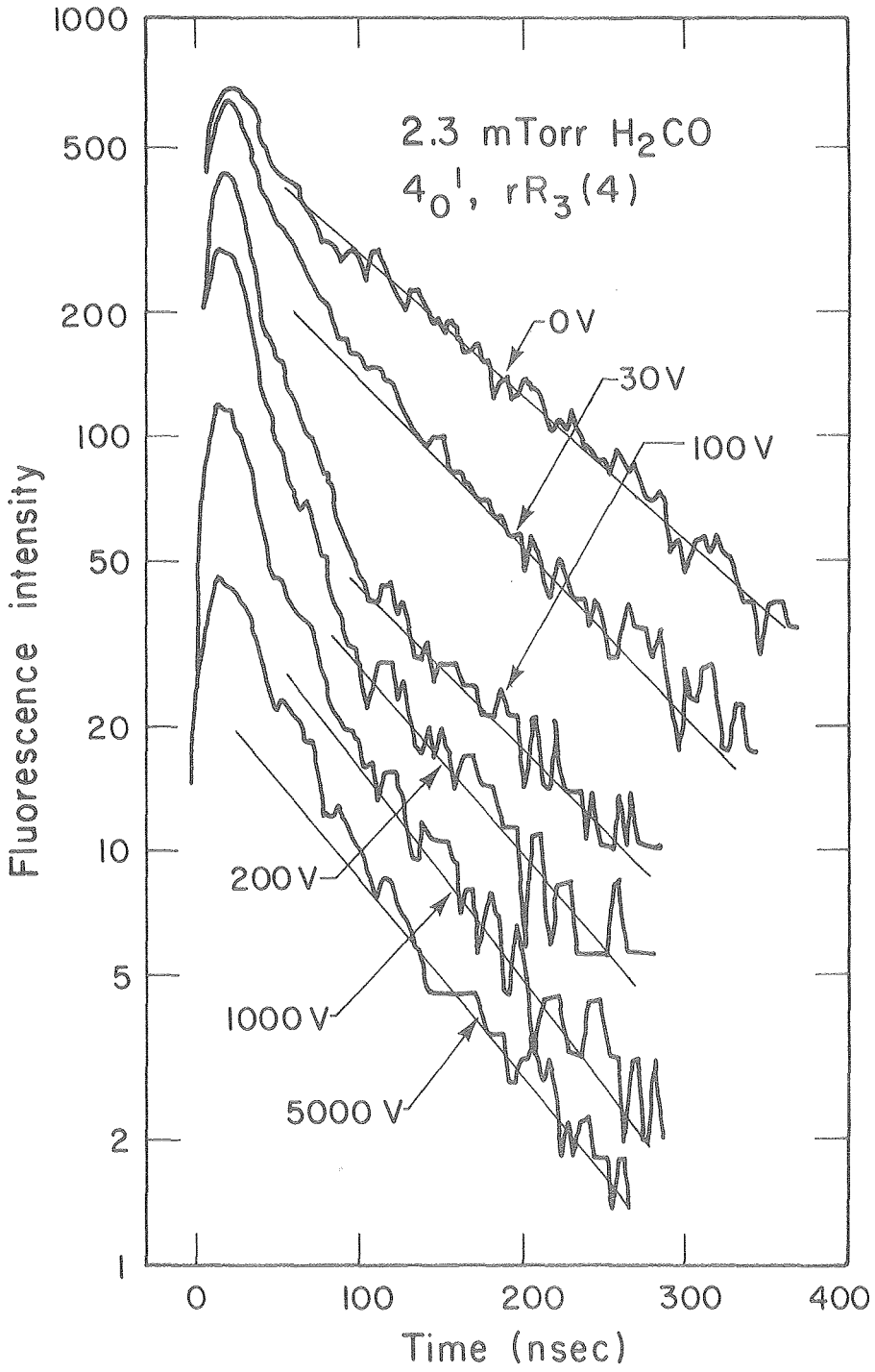

XBL 798-2714

Fig. 3.

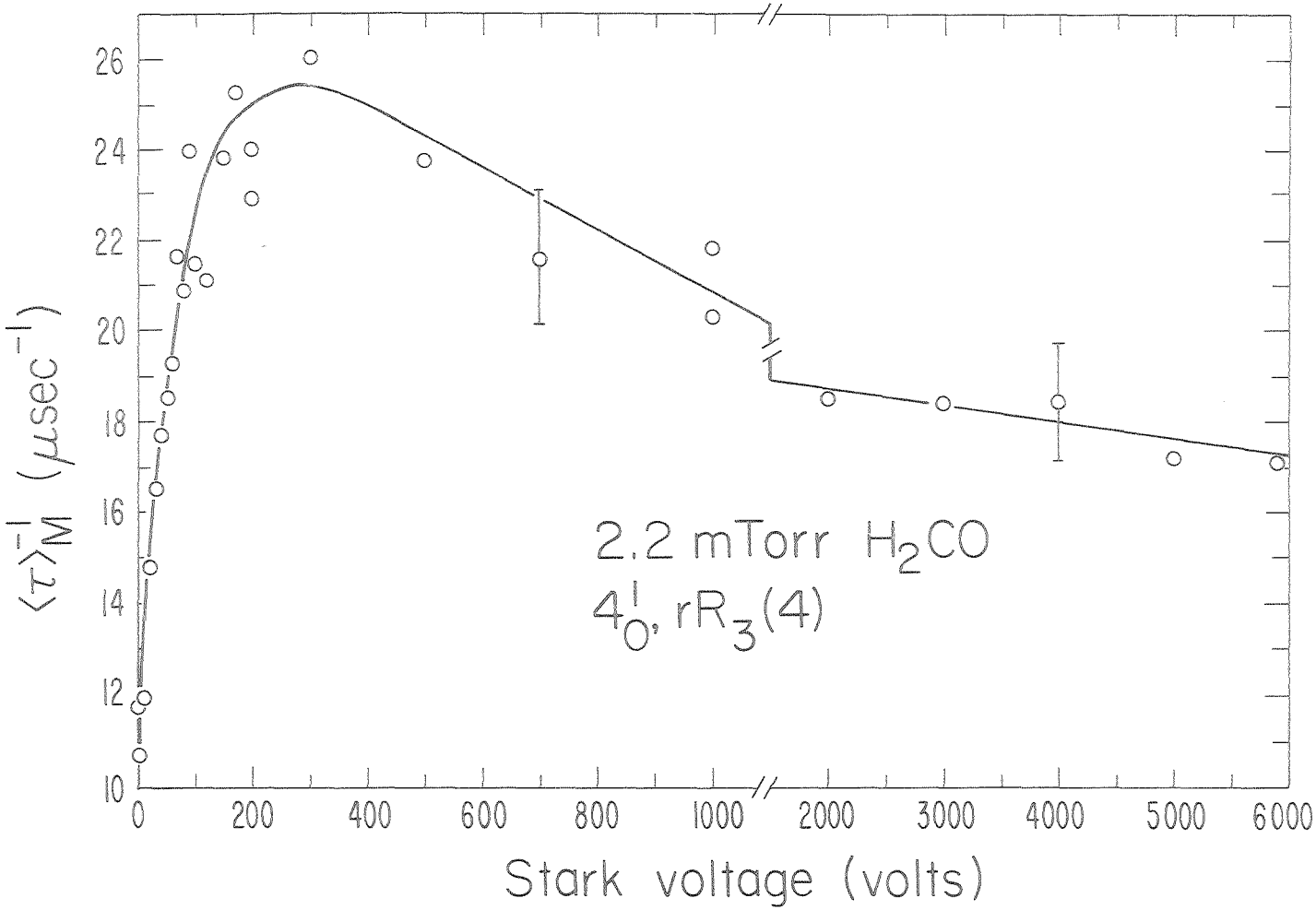

XBL 798-2707

Fig. 4.

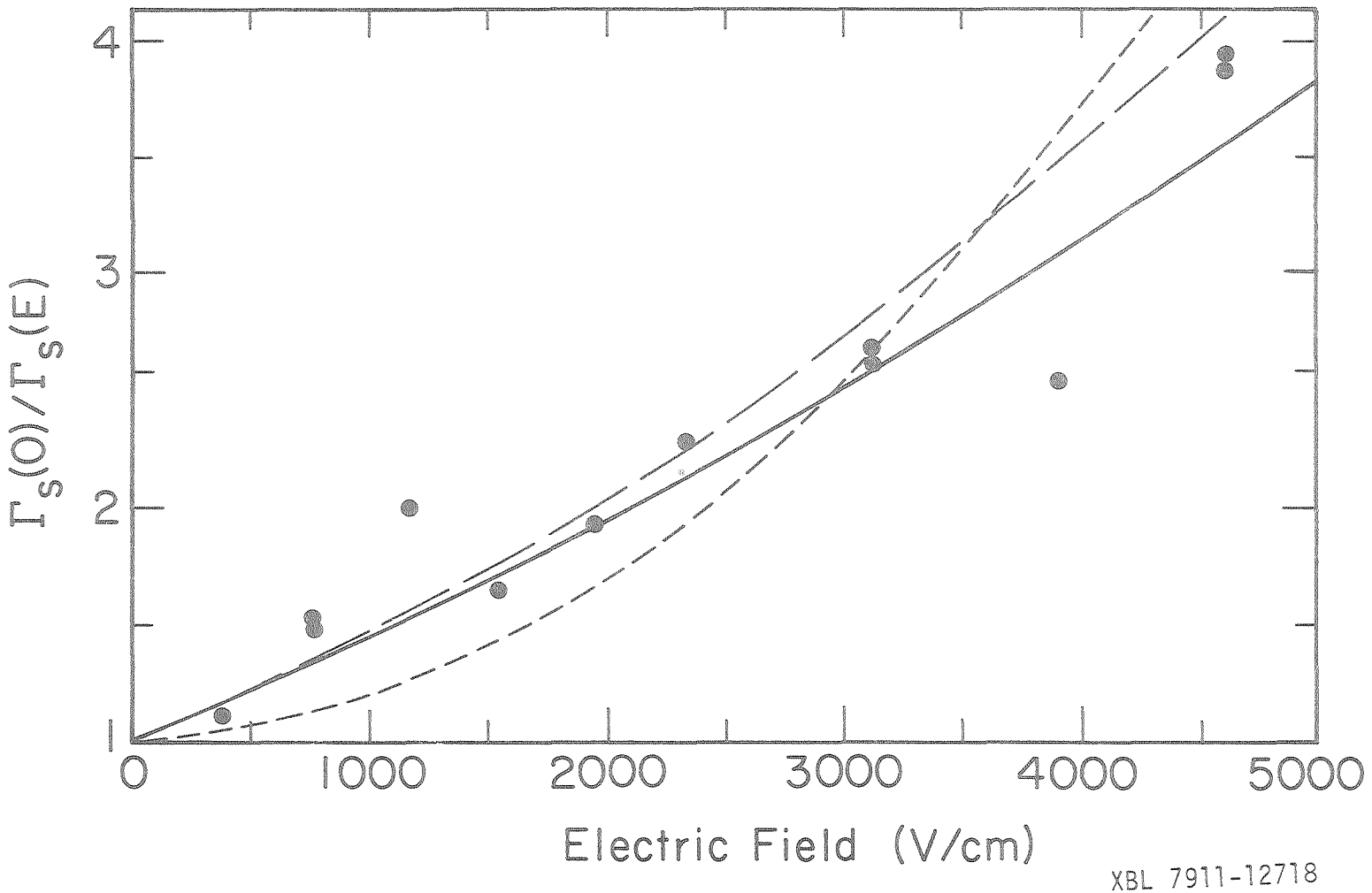
$T_s(0)/T_s(E)$
1
2
3
4
0
1000
2000
3000
4000
5000
Electric Field (V/cm)
XBL 7911-12718

Fig. 5.